

ANALYSIS OF THE FLOW CHARACTERISTIC INSIDE A HEATED AND
UNHEATED HORIZONTAL RIFLED TUBE

SOO POEY LAM

A thesis submitted in
fulfillment of the requirement for the award of the
Degree of Master of Mechanical Engineering

FACULTY OF MECHANICAL & MANUFACTURING ENGINEERING
UNIVERSITY OF TUN HUSSEIN ONN MALAYSIA

FEBRUARY 2012

ABSTRACT

Rifled tube which is one of the rough surface tube has been getting attention from researchers due to its ability to enhance the heat transfer. Previous researches on rifled tube has been done through experimental work. Therefore, numerical analysis by using commercial Computational Fluid Dynamics (CFD), Fluent® has been carried out to investigate the flow characteristic of the single phase flow in 2 meters long of horizontally rifled tube and smooth tube under heating condition and without heating condition at the outer wall. The rifled tube or also known as spiral internally ribbed tube that is used in this investigation has an outside diameter 45.0 mm and inside equivalent diameter of 33.1 mm while the smooth tube has an outside diameter 45 mm and inside diameter 34.1 mm. The working fluid that is used in this investigation is water. In this numerical analysis, realizable k-epsilon model has been chosen to solve the fully developed turbulence flow in the rifled tube and smooth tube. The result of the numerical analysis showed that there was swirling effect at the near-wall-region for both the case of the rifled tube under heating condition and without heating condition at the wall. The flow characteristic of the rifled tube in terms of pressure drop when there is no heat flux condition at the outer wall shows that the pressure drop in rifled tube is 1.69 – 1.77 folds than in the smooth tube. Meanwhile, when there is heating at the wall of the tubes, the pressure drop and heat transfer coefficient in rifled tube are about 1.67-2.0 times and 0.97-1.27 times respectively, than in smooth tube. The high pressure drop and Nusselt number in rifled tube is due to the helical rib in the rifled tube which not only has disturbed the flow but also causes swirling effect near the wall. As a result, the heat transfers from the wall to the flow near the wall region is enhanced. The present study also has proved that although the rifled tube produces high pressure drop but it is good in heat transfer enhancement through the ratio of heat flux to the pumping power.

ABSTRAK

Tiub berulir merupakan salah satu jenis tiub berpermukaan kasar yang mendapat perhatian daripada para penyelidik disebabkan keupayaannya meningkatkan proses pemindahan haba. Kebanyakan kajian terdahulu ke atas tiub ini dilaksanakan secara bereksperimen. Oleh itu, analisis secara kaedah berangka dengan menggunakan perisian komersial perkomputeran dinamik bendalir (CFD), iaitu *Fluent*® telah dilaksanakan untuk mengkaji ciri-ciri aliran fasa tunggal di dalam tiub berulir dan tiub licin yang masing-masing panjangnya 2 meter dengan keadaan tiub-tiub tersebut dikenakan haba dan tidak dikenakan haba pada permukaan luarnya. Tiub berulir atau juga dikenali sebagai tiub berusuk heliks yang digunakan di dalam eksperimen ini mempunyai garis pusat luar 45.0 mm dan garis pusat dalam setara 33.1 mm manakala tiub licin mempunyai garis pusat luar 45.0 mm dan garis pusat dalam 34.1 mm. Bendalir yang digunakan dalam ujikaji ini ialah air. Dalam analisis ini, model *realizable k-epsilon* telah dipilih untuk menyelesaikan aliran gelora di dalam tiub berulir dan tiub licin. Keputusan yang diperolehi daripada analisis menunjukkan terdapat kesan pusaran pada aliran air di kawasan mendekati dinding tiub bagi kedua-dua keadaan sama ada tiub-tiub itu dikenakan haba ataupun tidak dikenakan haba pada permukaan luar tiub. Ciri-ciri aliran air dari segi susutan tekanan di dalam tiub berulir dalam keadaan tiada haba dikenakan pada permukaan luar tiub menunjukkan susutan tekanan di dalam tiub berulir sebanyak 1.69 – 1.77 kali lebih daripada tiub licin. Semenata itu, apabila haba dikenakan di luar permukaan tiub berulir, susutan tekanan dan pekali pemindahan haba di dalam tiub berulir masing-masingnya adalah sebanyak 1.67 – 2.0 kali dan 0.97 – 1.27 kali lebih daripada tiub licin. Perbezaan ketara dari segi susutan tekanan dan nombor Nusselt aliran air di dalam tiub licin dan tiub berulir adalah disebabkan oleh rusuk heliks di dalam tiub

berulir yang bukan sahaja telah mengganggu aliran air malah telah menyebabkan kesan pusaran aliran air di kawasan mendekati dinding tiub. Akibatnya, ia mendorong kepada peningkatan pemindahan haba daripada dinding tiub kepada aliran air. Ujikaji ini melalui nisbah jumlah haba (yang dipindahkan) kepada kuasa pam yang dijana, telah membuktikan walaupun tiub berulir menghasilkan susutan tekanan yang tinggi, tetapi ia baik dari segi meningkatkan pemindahan haba.

CONTENT

TITLE	i
DECLARATION	ii
DEDICATION	iii
ACKNOWLEDGEMENT	iv
ABSTRACT	v
ABSTRAK	vi
CONTENT	viii
LIST OF TABLES	xii
LIST OF FIGURES	xiii
LIST OF SYMBOLS	xvii
LIST OF APPENDIXES	xix
CHAPTER 1 INTRODUCTION	1
1.1 Background of problem	1
1.2 Problem statement	3
1.3 Objectives	3
1.4 Scopes	4
1.5 Hypothesis	4
CHAPTER 2 LITERATURE REVIEW	5
2.1 Heat transfer enhancement technique	5

2.2	Surface roughness heat transfer enhancement technique	6
2.3	Two dimensional rib roughness	7
2.4	Rifled tube	9
2.5	Previous study	10
CHAPTER 3 SINGLE PHASE PRESSURE DROP IN THE RILFED TUBE		
UNDER NO HEATING CONDITION AT THE OUTER WALL		
3.1	Methodology	17
3.2	Geometry modeling	19
3.3	Pre-processing	21
3.3.1	Meshing	21
3.3.2	Boundary condition	23
3.4	Solving	26
3.4.1	Governing equation	26
3.4.2	Turbulence model	27
3.4.3	Flow solver	29
3.4.4	Pressure-velocity coupling method	30
3.4.5	Convergence criteria	31
3.4.6	Grid independent	32
3.5	Post-processing	34
3.5.1	Pressure drop	34
3.6	Results and discussion	35
3.6.1	Grid independence	35
3.6.2	Validation	37
3.6.3	Flow pattern	38
3.6.4	Pressure drop	40
3.6.5	Correlation of single phase friction factor	44

CHAPTER 4 SINGLE PHASE PRESSURE DROP AND HEAT TRANSFER IN
THE RILFED TUBE UNDER HEATING CONDITION AT THE OUTER WALL45

4.1	Methodology	45
4.2	Geometry modeling	47
4.3	Pre-processing	48
	4.3.1 Meshing	48
	4.3.2 Boundary condition	50
4.4	Solving	50
	4.4.1 Governing equation	51
	4.4.2 Turbulence model	51
	4.4.3 Energy model	52
	4.4.4 Flow solver	54
	4.4.5 Pressure-velocity coupling method	54
	4.4.6 Convergence criteria	54
	4.4.7 Grid independence	55
4.5	Post-processing	56
	4.5.1 Pressure drop	56
	4.5.2 Nusselt number	56
	4.5.3 Heat transfer enhancement characteristic	57
4.6	Results and discussion	58
	4.6.1 Grid independence	58
	4.6.2 Validation	61
	4.6.3 Flow pattern	63
	4.6.4 Pressure drop	65
	4.6.5 Temperature distribution	68

4.6.6	Pressure drop increase factor and heat transfer enhancement factor	72
4.6.7	Ratio of heat flux to pumping power	73
4.6.8	Correlation of single phase friction factor and heat transfer	75
CHAPTER 5 CONCLUSION		78
5.1	Summary	78
5.2	Recommendation for further research	79
REFERENCE		80
APPENDIX		84

LIST OF TABLES

2.1	Some example of the passive and active techniques. (Webb, R. L. & Kim, N. H., 2005)	6
2.2	The features between internally finned tube and rough tube. (Webb, R. L. & Kim, N. H., 2005)	9
3.1	The dimension of the rifled tube geometry parameters.	19
3.2	Percentage of different between numerically obtained pressure drop in the smooth tube at each level of number of cell.	36
3.3	Percentage of different between numerically obtained pressure drop in the rifled tube at each level of number of cell.	37
4.1	Percentage of different between numerically obtained pressure drop in the rifled tube at each level of number of cell.	59
4.2	Percentage of different between numerically obtained heat transfer coefficient in the rifled tube at each level of number of cell.	60
4.3	The percentage of different between smooth tube and rifled tube inner wall temperature.	71

LIST OF FIGURES

1.1	Rifled tube also known as helically internally ribbed tube.	2
2.1	Catalogue of roughness geometries. (Webb, R. L. & Kim, N. H., 2005)	7
2.2	Illustrations of different method on making two-dimensional roughness in a tube. (a) Integral transverse rib, (b) corrugated transverse rib, (c) integral helical rib, (d) helically corrugated, (e) wire coil insert, (f) different profile shapes of roughness (Webb, R. L. & Kim, N. H., 2005)	8
2.3	The front section view of a rifled tube.	10
3.1	The process flow of numerical analysis which is carried out on the rifled tube.	18
3.2	The geometry parameters of the rifled tube which is modeled in the Solidworks®.	19
3.3	A 3-dimensional fluid domain of the rifled tube which is modeled in the Solidworks®.	20
3.4	A typical hexahedral element with eight nodes (in black dote) which is used for storage of dependent variables. (Gambit® 2.4 electronic documentation)	21
3.5	The hexahedral mesh element is applied to the whole control volume of (a) smooth tube and (b) rifled tube.	22
3.6	The setting at the inlet for the smooth tube and rifled tube.	24
3.7	No slip boundary condition is applied on inner wall of the smooth tube and rifled tube.	25

3.8	The setting of the realizable k- ϵ model which is applied in the smooth tube and rifled tube case.	28
3.9	Pressure based solver has been selected for both of the smooth tube and rifled tube case.	30
3.10	The solution controls which have been applied in simulating the flow in the smooth tube and rifled tube.	31
3.11	Default convergence criteria for continuity, momentum and transport equations have been used applied on both smooth tube and rifled tube.	32
3.12	The inner wall of the smooth tube and rifled tube has been chosen to be adapted through Y+ adaption method in order to achieve grid independence.	33
3.13	The plotted graph shows that the obtained pressure drop in the smooth tube is grid independence to the number of cell.	35
3.14	The plotted graph shows that the obtained pressure drop in the rifled tube is grid independence to the number of cell.	36
3.15	Validation of the numerically obtained pressure drop in the smooth tube with calculated pressure drop.	38
3.16	The flow pattern in the smooth tube at $Re_D = 20000$.	39
3.17	The flow pattern in the rifled tube at $Re_D = 20000$.	40
3.18	The contour plot of the static pressure in the smooth tube at $Re_D = 20000$.	41
3.19	The contour plot of the static pressure in the rifled tube at $Re_D = 20000$.	42
3.20	Comparison of the numerical obtained pressure drop in the smooth tube and rifled tube.	43
3.21	Comparison of the numerical obtained friction factor in the smooth tube, calculated friction factor in the smooth tube and rifled tube.	43
3.22	A correlation for single phase friction factor in the rifled tube has been proposed.	44
4.1	The process flow of numerical analysis which is carried out on the rifled tube and smooth tube.	46
4.2	The geometry modeling of the rifled tube with wall	47

4.3	The geometry modeling of the smooth tube.	48
4.4	The smooth tube with wall meshed with hexahedral element.	49
4.5	The rifled tube with wall meshed with hexahedral element.	49
4.6	The thermal effects in the k- ϵ model is being checked.	52
4.7	Energy equation has been enabled so that it is solved by the Fluent.	53
4.8	Default convergence criteria for continuity, momentum and transport equations have been used applied on both smooth tube and rifled tube.	55
4.9	The plotted graph shows that the obtained pressure drop in the smooth tube is grid independence to the number of cell.	59
4.10	The plotted graph shows that the obtained heat transfer coefficient in the smooth tube is grid independence to the number of cell.	60
4.11	Validation of the numerically obtained pressure drop in the smooth tube with calculated pressure drop.	62
4.12	Validation of the numerically obtained heat transfer coefficient in the smooth tube with calculated heat transfer coefficient.	63
4.13	The flow pattern in the smooth tube at $Re_D = 20000$.	64
4.14	The flow pattern in the rifled tube at $Re_D = 20000$.	65
4.15	The contour plot of the static pressure in the smooth tube at $Re_D = 20000$.	66
4.16	The contour plot of the static pressure in the rifled tube at $Re_D = 20000$.	67
4.17	Comparison of the numerical obtained pressure drop in the smooth tube and rifled tube.	68
4.18	The temperature distribution in smooth tube.	70
4.19	The temperature distribution in the rifled tube.	70
4.20	The inner wall and outlet wall temperature between smooth tube and rifled tube.	71
4.21	Pressure drop increase factor and heat transfer enhancement factor in rifled tube.	73
4.22	The ratio of heat flux to pumping power between smooth tube and rifled tube.	74

- 4.23 A correlation for single phase friction factor in the rifled tube has been proposed. 76
- 4.24 A correlation for single phase heat transfer in the rifled tube has been proposed. 77

LIST OF SYMBOLS

$C_{1\varepsilon}, C_{2\varepsilon}, C_\mu$	constants of the k - ε model
c_p	specific heat capacity of fluid, J/kg·K
D_{in}	inner diameter, m
D_{eq}	equivalent inner diameter, m
$D_{in,min}$	minimum inner diameter, m
$D_{in,max}$	maximum inner diameter, m
e	rib height, m
E	heat flux, W/m ²
f	friction factor
h	heat transfer coefficient, W/m ² ·K
k_{eff}	effective thermal conductivity, W/m·K
k_t	turbulent thermal conductivity, W/m·K
k_f	fluid thermal conductivity, W/m·K
L	lead, m
L_H	heated length, m
L_t	length of tube, m
\dot{m}	mass flow rate, kg/s
Mn	Manganese
N	number of ribs
Nu	Nusselt number
n	coordinate direction perpendicular to a surface
p	pitch, m
P	pressure, Pa
ΔP	pressure drop, Pa

Pr	Prandtl number
q'	input heat flux, W/m^2
Re	Reynolds number
S_{mi}	source term in i direction
Si	Silicon
t	time, second
T_{in}	inlet temperature, K
T_{out}	outlet temperature, K
u, v, w, u_i, u_j	mean velocity components, m/s
u', v', w', u'_i, u'_j	turbulent fluctuating velocity component, m/s
u_w	mean velocity at wall, m/s
u	fluid flow velocity, m/s
\vec{V}	velocity vector, m/s
w	rib width, m
\dot{W}_P	pumping power, W/m^2
x_i, x_j	Cartesian coordinate
ρ	density of fluid, kg/m^3
θ	helical angle, $^\circ$
μ, μ_T, μ_{eff}	laminar, turbulent and effective viscosities, $\text{kg}/\text{m}\cdot\text{s}$
$\sigma_k, \sigma_\epsilon$	turbulent Prandtl numbers for k - ϵ model
γ	ratio of heat flux to pumping power, $(\text{W}/\text{m}^2)/\text{W}$

LIST OF APPENDIXES

A	The contour of static pressure for Reynolds number ranging from 20000 to 140000 under heating condition at the outer wall of 2m long smooth tube.	84
B	The contour of static pressure for Reynolds number ranging from 20000 to 140000 under heating condition at the outer wall of 2m long rifled tube.	88
C	The contour of static pressure for Reynolds number ranging from 20000 to 140000 under no heating condition at the outer wall of 2m long smooth tube.	92
D	The contour of static pressure for Reynolds number ranging from 20000 to 140000 under no heating condition at the outer wall of 2m long rifled tube.	96
E	The velocity vector (in cross section view) of the flow for Reynolds number ranging from 20000 to 140000 under no heating condition at the outer wall of 2m long smooth tube.	100
F	The velocity vector (in cross section view) of the flow for Reynolds number ranging from 20000 to 140000 under no heating condition at the outer wall of 2m long rifled tub.	104
G	The velocity vector (in cross section view) of the flow for Reynolds number ranging from 20000 to 140000 under heating condition at the outer wall of 2m long smooth tube.	108
H	The velocity vector (in cross section view) of the flow for Reynolds number ranging from 20000 to 140000 under	

	heating condition at the outer wall of 2m long rifled tube.	112
I	The static temperature (in cross section view) of the flow for Reynolds number ranging from 20000 to 140000 under heating condition at the outer wall of 2m long rifled tube.	116
J	The static temperature (in cross section view) of the flow for Reynolds number ranging from 20000 to 140000 under heating condition at the outer wall of 2m long smooth tube.	120
K	Calculation of the rifled tube hydraulic diameter.	124
L	The Fluent software code which is used to predict the flow characteristic in the smooth tube under no heating condition at the outer wall.	127
M	The Fluent software code which is used to predict the flow characteristic in the rifled tube under no heating condition at the outer wall.	134
N	The Fluent software code which is used to predict the flow characteristic in the smooth tube under heating condition at the outer wall.	142
O	The Fluent software code which is used to predict the flow characteristic in the rifled tube under heating condition at the outer wall.	153

CHAPTER 1

INTRODUCTION

1.1 Background of problem

In light of environment issues, many heat transfer enhancement techniques have been developed and used for increasing heat transfer in heat exchanger such as condensers, evaporators, boilers and other heat exchanger used in various commercial and industrial applications. The advantages of the enhancement techniques is that it reduces the thermal resistance in a conventional heat exchanger by promoting higher convective heat transfer coefficient with or without surface area increases. Heat transfer enhancement techniques can be classified into three categories; active, passive and compound heat transfer enhancement techniques (Webb, R. L. & Kim, N. H, 2005). Among those three categories, a passive heat transfer enhancement technique is more practical use and is easily implemented as compared with active and compound heat transfer enhancement techniques. Besides that, it also does not consume any external power while active and compound enhancement techniques require addition of external power to bring about the desired flow modification. Passive heat transfer enhancement techniques use surface modification or an additional device incorporated into the equipment. The existing boundary layer is disturbed and the heat transfer performance is improved, usually

with an increase in flow friction and pressure drop. Typical examples of this type of techniques are surface roughness, displaced promoters and vortex generators (Webb, R. L. & Kim, N. H, 2005). Surface roughness introduced through knurling or threading or formed by repeated ribs, promotes enhancement through the disturbance of the sublayer that is close to the surface. One of these type products is the rifled tube.

Rifled tube is also known as ribbed tube or helically internally ribbed tube (Cheng, L. X. & Chen, T. K., 2007). The shape of rifled tube is as shown in Figure 1.1.

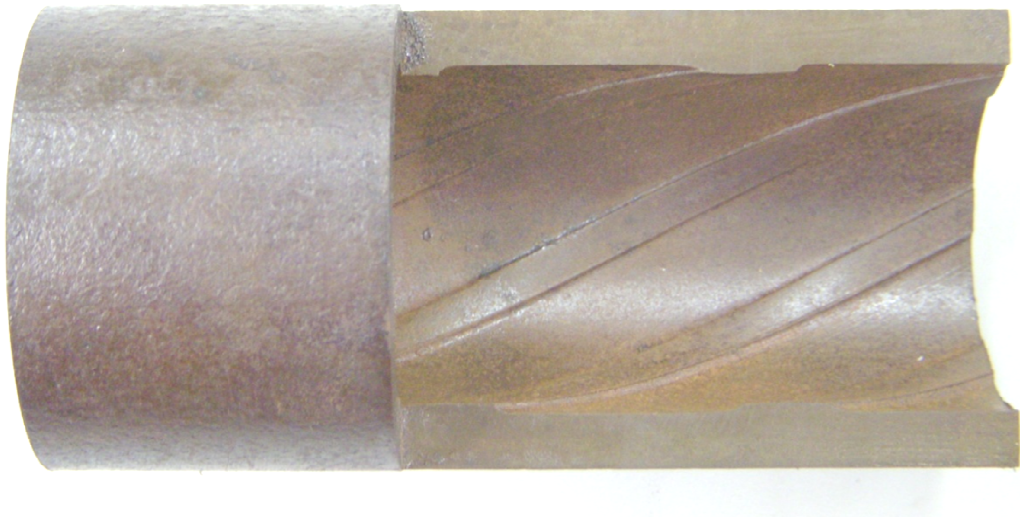


Figure 1.1 Rifled tube also known as helically internally ribbed tube.

The advantage of the rifled tube compared to smooth tube is that it will cause the swirling effect in the flow. They also act like a roughness element mixing up the flow in the viscous sublayer (Kundu, P. K. & Cohen, I. M., 2004). Besides that due to its inner geometry shape, flow is thrown outwards to the tube wall as a result of centrifugal action. Thus, creates a secondary flow or also known as helical flow or a swirl flow at the near wall region. This helical flow at the tube periphery superimposes on the main axial flow. This effect enhances wall wetting and prevents critical heat transfer occurrence even under high steam void fraction conditions and

lower critical heat flux. As a result, this type of tube would not easily burnout and can be used under much higher operating condition than the smooth tube.

1.2 Problem statement

Literatures in hand have showed that many of the research regarding rifled tube are more on experiment work, and none of them predicting the flow characteristic of the rifled tube through numerical method. Thus, in the present study, numerical analysis by using commercial Computational Fluid Dynamic (CFD) software, i.e. Fluent® shall be used to predict the flow characteristic in the rifled tube. The use of the commercial CFD software to model the fluid flow inside the rifled tube is very useful in this research as it will save time and cost in setting up an experiment.

1.3 Objectives

- a) To study the flow pattern and pressure drop inside the rifled tube when there is no uniform heating at the outer wall.
- b) To study the flow pattern, pressure drop and Nusselt number of the rifled tube when there is a uniform heating at the outer wall.

1.4 Scopes

- a) Computational Fluid Dynamics (CFD) is used to compute the flow characteristic of the rifled tube.
- b) Only single phase flow is used to determine the flow characteristic in the smooth tube and rifled tube.
- c) Water is used as working fluid.
- d) Smooth tube and rifled tube are assumed to be placed horizontally in this research.

1.5 Hypothesis

- a) Computational Fluid Dynamics (CFD) able to predict the flow pattern, pressure drop and heat transfer coefficient inside the rifled tube.
- b) The pressure drop inside the rifled tube is higher than in the smooth tube.
- c) The heat transfer coefficient inside the rifled tube is higher than in the smooth tube.
- d) The inner wall temperature of the rifled tube is lower than in the smooth tube.

CHAPTER 2

LITERATURE REVIEW

2.1 Heat transfer enhancement technique

Generally, heat transfer enhancement technique can be classified into three groups that are passive techniques, active techniques and compound techniques which is combination of two or more passive and active techniques. Passive techniques do not require any external power and this techniques employ special surface geometries or fluid additives for enhancement. On the other hand, active techniques required external power such as electric or acoustic fields and surface vibration (Webb, R. L. & Kim, N. H., 2005). Table 2.1 shows example of the passive and active techniques.

Table 2.1 Some example of the passive and active techniques. (Webb, R. L. & Kim, N. H., 2005)

Heat transfer enhancement technique	Example
Passive techniques	Coated surfaces Rough surfaces Extended surfaces Displaced insert Swirl flow Coiled tubes Surface tension Additives for liquids Additives for gases
Active techniques	Mechanical aids Surface vibration Fluid vibration Electrostatic fields Injection Suction Jet impingement

2.2 Surface roughness heat transfer enhancement technique

In the surface roughness category, there are three type of roughness or internal surface that is three dimensional roughness (uniform roughness), ridged-type two dimensional roughness (repeated ribs) and grooved-type two dimensional roughness (Webb, R. L. & Kim, N. H., 2005). Figure 2.1 shows the basic roughness geometries.

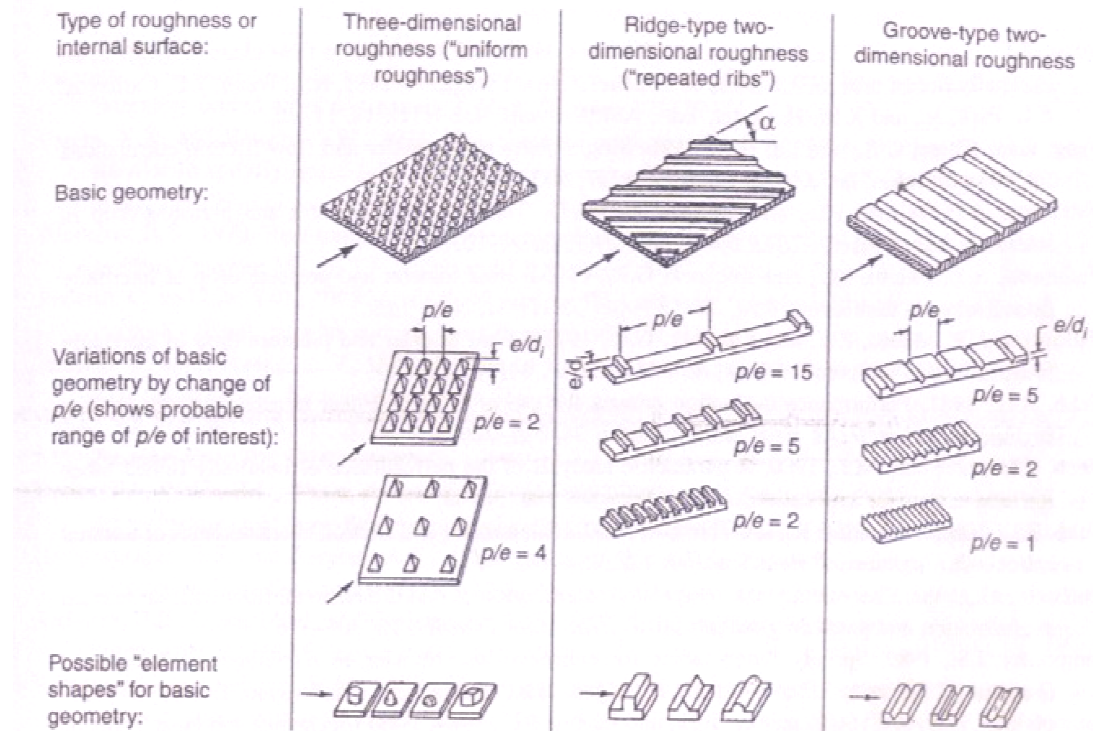


Figure 2.1 Catalogue of roughness geometries. (Webb, R. L. & Kim, N. H., 2005)

For any basic type of roughness family, the key dimensionless variables are the dimensionless roughness height (e/d_i), the dimensionless roughness spacing (p/e), the dimensionless rib width (w/e), and the shape of roughness element (Webb, R. L. & Kim, N. H., 2005). The symbol of e represents rib height, d_i represents the tube inner diameter, p represents the rib spacing and w represents the rib width.

2.3 Two dimensional rib roughness

There are many variants of two dimensional roughness. As shown in Figure 2.2, the two dimensional roughness can be transverse ribs which the ribs are normal to the flow, helical rib roughness with helical angle less than 90° and the roughness element

may be integral to the base surface or they may be in the forms of wire coil inserts (Webb, R. L. & Kim, N. H., 2005).

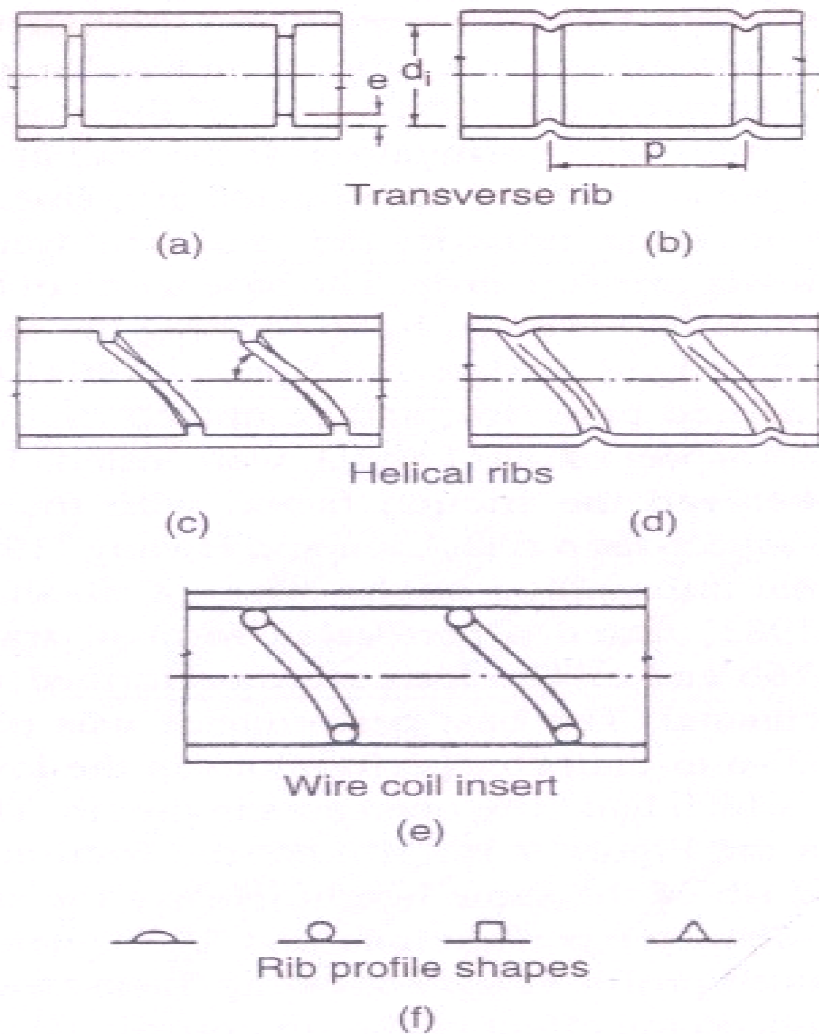


Figure 2.2 Illustrations of different method on making two-dimensional roughness in a tube. (a) Integral transverse rib, (b) corrugated transverse rib, (c) integral helical rib, (d) helically corrugated, (e) wire coil insert, (f) different profile shapes of roughness (Webb, R. L. & Kim, N. H., 2005)

One may find out that the two dimensional roughness especially the rib roughness are quite similar to internally finned tube which is an example of extended surfaces. According to Webb, R. L. & Kim, N. H. (2005), to fall within the internal

fin classification requires that no flow separations exist on the internal fin. Contrast to the internally finned tube, the flow separation is a key feature of the enhancement mechanism of rough tubes. Table 2.2 shows the some of the difference feature between internally finned tube and rough tube.

Table 2.2 The features between internally finned tube and rough tube. (Webb, R. L. & Kim, N. H., 2005)

Feature	Internally finned tube	Rough tube
Flow separation	Do not exist on the internal fin	Exist on the internal fin or rib
Surface area	Significant increase	Not significant increase
Helical angle	small (less than 15°)	Larger (less than 90°)
Dimensioless roughness height, e/d_i	Larger due to fin height	Smaller

2.4 Rifled tube

Rifled tube or also known as helically ribbed tube or also commercially known as Turbo-Chil™ tube is one of the passive techniques. It is one of the examples of two dimensional rib roughness. It is termed as ‘rifled tube’ due to its similarity to the rifled barrel in a firearm (Zarnett, G. D. & Charles, M. E., 1969).

There are several important geometry parameter in the rifled tube and they are maximum inside diameter ($D_{in,max}$), helical angle (θ), number of rib (N), rib height (e), rib width (w), lead (L) and element axial pitch (p) as shown in Figure 2.3. All of these parameters can be related as follow (Webb, R. L. & Kim, N. H., 2005);

$$\text{Pitch, } p = \frac{\pi D_{in,max}}{N \tan \theta} \quad (1)$$

$$\text{Number of starts, } N = \frac{L}{p} \quad (2)$$

(Note: the lead is measured almost same like measuring the pitch but the difference is the lead is measured from a rib until the end of cycle of the rib.)

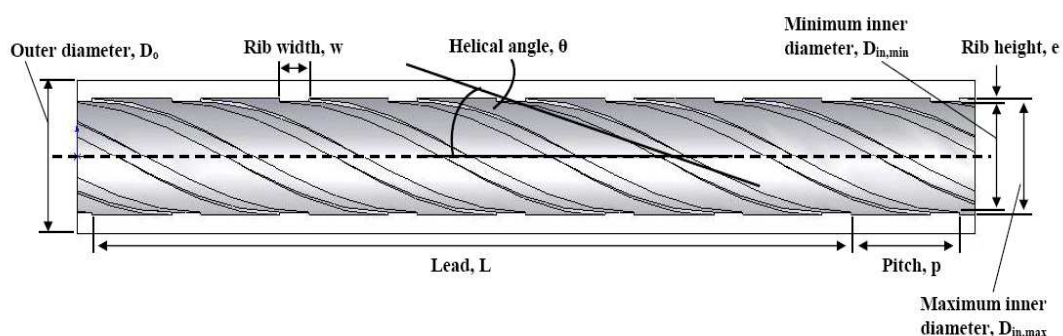


Figure 2.3 The front section view of a rifled tube.

2.5 Previous study

Smith, J. W. et. al. (1968) had experimentally measured the turbulent heat transfer and temperature profiles in a rifled pipe. The rifled pipe was made by fitting snugly the continuous spiral rib inside a smooth brass tube which had the inner diameter of 2.058 inch. The continuous spiral rib was created from 0.25 inch x 0.25 inch copper bar with pitch to diameter ratio of 2.58. From the experimental data, the authors had summarized that the rifled pipe had resulted in greater than two fold increases in Stanton number, St , but with a proportionate increase in friction factor, C_f , which was dependant on Reynolds number. The temperature profiles showed that the rifling had reduced the resistance to heat transfer in the turbulent core which in the end the rifled tube offered a much better heat transfer efficiency than in the smooth tube. Due to relatively uniform temperature profiles in the rifled tube, the authors had

suggested that the application of the rifled tube in tubular type reactors to ensure uniform temperature distribution.

Zarnett, G. D. & Charles, M. E. (1969) had carried out experimental work to observe the flow patterns of two phase flow in horizontal tubes fitted with internal spiral tubes (rifled tube) which their pitch to diameter ratios is 1.57 and 2.79 respectively. Besides that, comparison of single phase friction factor between smooth tube and the two rifled tubes also have been done which showed that the friction factors for the two rifled tubes were larger than the smooth tube. Correlations for friction factor also have been established for the two rifled tubes.

Webb, R. L. et. al. (1971) had developed the heat transfer and friction correlations for turbulent flow in repeated-rib roughness tube. In this experiment, the rib inside the repeated-rib roughness tube is positioned in transverse direction with value of relative roughness (e/D) ranging between 0.01 to 0.04 while the relative rib spacing (p/e) ranging between 10-40. The e represent the rib height, D represent the maximum inner diameter of tube and p represent the pitch between the ribs. From this experiment, the friction data of the experiment had been well correlated using law of the wall similarity with a logarithmic velocity distribution. On the other hand, the heat momentum transfer analogy which was based on law of the wall similarity, was found to be superior in accounting for the effect of Prandtl number. The correlations which was proposed by the authors specifically apply to ribs of rectangular cross-section, whose thickness is small relative to the rib spacing.

Han, J. C. et. al. (1978) had carried out investigation on rib-roughened surface to determine the effect of rib shape, angle of attack and pitch to height ratio on friction factor and heat transfer. In this experiment, the rib roughened surface is consist of symmetry and staggered ribs on a parallel plate. The flow will flow through this parallel plates and the experimental result was obtained. It is noted that the friction factor is decreases with angle of attack decreasing. Further decreasing in angle of attack, will cause the heat transfer and the friction approaching the smooth wall case. The thermal hydraulic performance of the tested ribs was at optimum when angle of attack near 45° .

Iwabuchi, M. et al. (1982) had studied the heat transfer characteristics of rifled tube in the near critical pressure region. In this experiment, smooth tube and rifled tube were tested to study their heat transfer characteristic. The smooth tube

was made of 1.25Cr-0.5Mo steel tube of outside diameter, 28.6mm. The rifled tube with 4 ribs had an inner diameter 17.7mm, rib height 0.83mm and helix angle 30° . In the test section, their circumferentially heated angles were 360° and 180° respectively. The experiment result shows that when pressure exceeds 20.6MPa, the swirl effect will diminishes and CHF condition appears even in the sub cooled region. However, the wall temperature rise is suppressed to a comparatively lower level.

Köhler, W. & Kastner, W. (1986) had investigated the effect of internal rifling on heat transfer and pressure loss under high pressure in rifled tube. The experimental parameters like pressure, mass velocity, and heat flux are ranging from 50-220 bar, 500-1500 kg/m²s, and 0-600kW/m² respectively. The flow orientation in this experiment is vertical up flow. The rifled tube that is used in this experiment have outer diameter, 25.4 mm, equivalent inner diameter, 13.25mm, number of ribs, 4, rib width, 3.5mm, rib height 0.775mm and helix angle 58° . The rifled tube is made of SA-213 GRADE T11 (ASME). In the heat transfer investigation, the internal rifling had caused the boiling crisis and post Critical Heat Flux (CHF) regime shift towards higher steam qualities comparing to smooth tube. The maximum wall temperature is much lower in the rifled tube than smooth tube. The pressure loss in the rifled tube also had been investigated for single phase and two phase flow which shows two folds than the smooth tube. It is found out that the thermal non-equilibrium in the unwetted region does not occurred (due to swirl flow) in the rifled tube.

Henry, F. S. & Collins, M. W. (1991) had numerically predicted the flow over transverse and helically ribbed cylinder by using FLOW3D. In this simulation, the authors had considered five ribbed geometries which had number of start ranging from 0 to 30, rib angle ranging from 0° to 59.767° and rib width ranging from 0.8609mm to 0.4335mm. In all the ribbed geometries, the inner cylinder diameter was 39.44mm, outer cylinder diameter was 98.09mm, rib height 1.13mm, and rib pitch 7.29mm. The result of pressure drop and flow pattern in the transverse and helically ribbed were then being compared with smooth tube which was assumed to have inner diameter 39.44mm and outer diameter 98.09mm. In the FLOW3D setting, standard k- ϵ model was employed together with wall functions at the solid boundaries. Grid refinement was also carried out in order to improve the pressure

drop result. From the simulation, the authors had summarized that there are no regions of separation and recirculation in turbulent flow over the helical ribbed geometry except for very acute rib angles, i.e. less than 19° . Due to substantial increase in the magnitude of the near-wall velocities in the inter-rib channel of the helical ribbed cylinder, the 'hot spot' or the critical heat flux at the wall region would be less likely to be occurred. The authors also suggested that the standard k- ϵ model is less efficient in predicting swirling flow which caused the difference between the experimental data and the simulation results. It also appeared that the use of wall function for the ribbed geometry considered may not be suitable to be used.

Almeda, J. A. & Souza Mendes, P. R. (1992) had experimentally investigated the local and average transport coefficients for the turbulent flow in internally ribbed tubes. The investigation encompassed entrance region results, fully developed results and local results. In this experiment, the authors had investigated the effect of the rib height and rib spacing in the ribbed tube to the pressure drop which it had found out that the friction factor in the ribbed tube is very sensitive to the dimensionless rib height, H/D and not as sensitive to the pitch P/H . It is also interesting to found out that the heat transfer enhancement increased with Re when H/D is less than 0.02 ($H/D < 0.02$) and vice versa. At $P/H = 8$, there was no additional gain in heat transfer enhancement if the rib height was increasing beyond $H/D = 0.05$. What is lack of this experiment is that the authors did not further investigate the ratio of pumping power to the heat transfer.

Weisman, J. et al. (1994) had carried out an experimental examination on two phase flow patterns and pressure drop in single and double helically ribs. In this experiment, helical wire ribs have been inserted into two tubes which had the diameter of 2.54cm and 5.10cm, respectively. The helical wire ribs had the height of 0.32, 0.64 and 1.27cm, while the helical twisted ratio are 1.2, 2.1, 2.3 and 2.5. It is concluded that when a minimum flow velocity is exceeded, not only swirling occurred, the enhancement of the critical heat flux would also occurred. The authors had proposed correlations for predicting the onset of swirling annular flow which can be used for air-water systems flowing in tubes with diameter between 1cm - 5cm and where the liquid velocity is in range between 0.1m/s and 0.5m/s while the gas velocity is in range between 0.2m/s and 25m/s.

Cheng, L. X. & Chen, T. K. (2001) had conducted experimental work of flow boiling heat transfer and two-phase flow frictional pressure drop in a vertical rifled tube and smooth tube under the condition of 0.6 MPa. The rifled tube that was used in the experiment had an outside diameter 22mm, average inner diameter 11.6mm rib width 5.5mm, rib height 0.4mm - 0.6mm and rib pitch 3.5mm. Nonetheless, the outside and inside diameter of the smooth tube are 19mm and 15mm. The results of the experiment had shown that the flow boiling heat transfer coefficient and two-phase frictional pressure drop in rifled tube were 1.4 - 2.0 times and 1.6 - 2.0 times, respectively than in the smooth tube. It was interesting to note that the superheat wall temperatures in the rifled tube are smaller than in the smooth tube under equal heat fluxes and equal mass fluxes. The authors had also found out that the flow boiling heat transfer coefficient would increase if the mass flux increase, but the pressures had little effect on the flow boiling heat transfer coefficient. Correlations of flow boiling heat transfer coefficient and two-phase frictional pressure drop in the rifled tube also had been proposed.

C. H. Kim et al. (2005) had evaluated the critical heat flux (CHF) performance for flow boiling of R134a in vertical uniformly heated smooth tube and rifled tube. In this experimental work, a four head and six-head rifled tube with outer diameter 22.59mm and minimum inner diameter ranging between 15.22mm - 15.39mm had been used under outlet pressures of 13, 16.5 and 23.9 bar, mass fluxes of 285 - 1300kg/m²s and inlet subcooling temperature ranging 5 - 40°C. It is concluded that the CHF enhancement in the rifled tube had been enhanced 40% - 60% than in the smooth tube. The CHF enhancement not only depends on the mass flux and pressure, but there is also a critical helical angle and critical velocity to get the CHF enhancement. The author had explained the CHF enhancement by using the relative velocity of vapor and it is interesting to note that when the flow pressure is near critical pressure, the helical angle is above 70° and the velocity is below 0.3m/s, the centrifugal acceleration will be decreased. As a result, the flow inside the rifled tube would be ceased to follow the ribs and the swirling flow is diminished.

Cheng, L. X. & Chen, T. K (2006) had carried out an experimental investigation on single phase flow heat transfer and friction pressure drop in a rifled tube and smooth tube. The rifled tube that is used in this experiment has an outside diameter of 22mm and maximum inner diameter 11mm while the smooth tube has an

outside diameter 19mm and inside diameter of 15mm. Both tube were uniformly heated by passing an electrical current along the tubes with a heated length 2500mm. the working fluid that was used in this experiment are water and kerosene with experimental Reynolds number is in the range $10^4 - 5 \times 10^4$ and $10^4 - 2.2 \times 10^4$ respectively. In order to ensure the experiment apparatus set up is reliable, the result of the experimental heat transfer coefficient and friction pressure drop had been compared with calculated one. The errors between experimental and calculated for heat transfer coefficient and friction pressure drop are within 6% and 8% respectively. The experimental results for heat transfer coefficient and friction pressure drop of water and kerosene in the rifled tube and smooth tube were compared. For water, the heat transfer coefficient and friction pressure drop of the rifled tube were improved by a factor of 1.2-1.6 times and 1.4 to 1.7 times respectively than the smooth tube. On the other hand, the heat transfer coefficient and friction pressure drop of kerosene in the rifled tube were also improved by a factor of 2 to 2.7 and 1.5 to 2 respectively as compared with those of the kerosene in the smooth tube. Besides that, the running cost for rifled tube also is lower than the smooth tube. The author had proposed correlations for Nusselt number and friction pressure drop of water and kerosene in the rifled tube. For water this correlations are applicable to the conditions in the range of test parameters $1.1 \leq Pr \leq 7$ and $10^4 \leq Re \leq 5 \times 10^4$, while for kerosene $1.6 \times 10^3 \leq Pr \leq 3.4 \times 10^4$ and $10^4 \leq Re \leq 2.2 \times 10^4$.

Cheng, L. X. & Chen, T. K. (2007) had calculated the two-phase pressure drop in a vertical rifled tube by using Friedel model and two-phase homogeneous model. An experiment was carried out to validate the pressure drop obtained from those models. It shows that the frictional pressure drop in the rifled tube was 1.6-2.7 times greater than in the smooth tube.

Tucakovic, D. R. et al. (2007) developed a computer code by using FORTRAN to simulate the influence of the rifled tube on thermal-hydraulic parameter such as working fluid flow rate, steam void fraction, circulation number, circulation velocity, and critical heat flux in a large steam boiler and the effect was discussed.

Yanaoka, H. et al. (2007) had carried out numerical simulation of separated flow transition and heat transfer around a two-dimensional rib mounted in a laminar boundary layer. The shear layer that separates at the leading edge of the rib becomes

unstable downstream and rolls up into a two-dimensional vortex. The instability of the separated shear layer is due to the Kelvin-Helmholtz instability. The heat transfer is low behind the rib but become active around the reattachment flow region due to the influence of the large-scale vortex generated by the transition of the separated shear layer.

Lee, S. K. & Chang, S. H. (2008) had studied experimentally the post dry-out with R-134a upward flow in smooth tube and rifled tube. The authors had used three type of rifled tube which had 4 head, helix angle 60° and maximum inside diameter of 17.04mm with an average volume based inner diameter of 16.49mm, 16.05mm and 16.79mm, respectively. From these three types of rifled tube, the authors then had examined the effects of rib geometry and compared with the smooth tube. The smooth tube that was used in the study had an average inner diameter of 17.04mm and outside diameter of 22.59mm. It is found out that the wall temperature of the rifled tube in the post-dryout region were much lower than in the smooth tube. As a result, the thermal non-equilibrium in rifled tube was lowered which was due to the swirling flow caused by the ribs in the rifled tube. The authors had also proposed heat transfer correlation for rifled tube as a function of rib height and rib width.

CHAPTER 3

SINGLE PHASE PRESSURE DROP IN THE RILFED TUBE UNDER NO HEATING CONDITION AT THE OUTER WALL

3.1 Methodology

The methodology of the present study can be divided into four stages of process flow which are geometry modeling, pre-processing, processing and post-processing as shown in the flow chart in Figure 3.1.

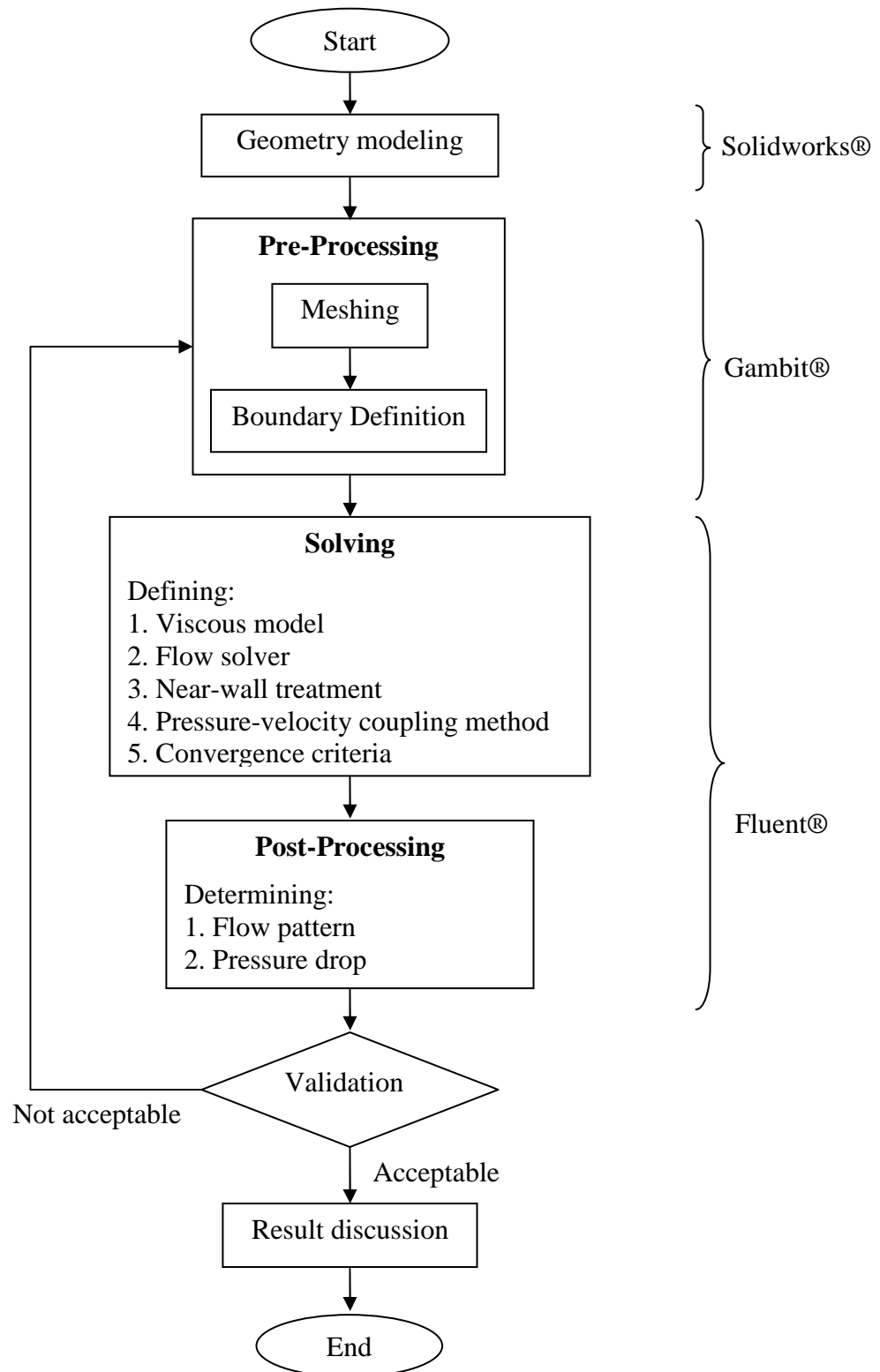


Figure 3.1 The process flow of numerical analysis which is carried out on the rifled tube.

3.2 Geometry modeling

The dimension of the rifled tube geometry parameters which will be modeled is as shown in Table 3.1. The dimensions of the rifled tube is based on Cheng, L. X. & Chen, T. K. (2006) with some modifications on the value of the dimensions. There are two inner diameters in the rifled tube, i.e. maximum inner diameter and minimum inner diameter. The equivalent inner diameter of the rifled tube has been determined by using following equation;

$$D_{eq} = \frac{D_{in,max} + D_{in,min}}{2} \quad (3)$$

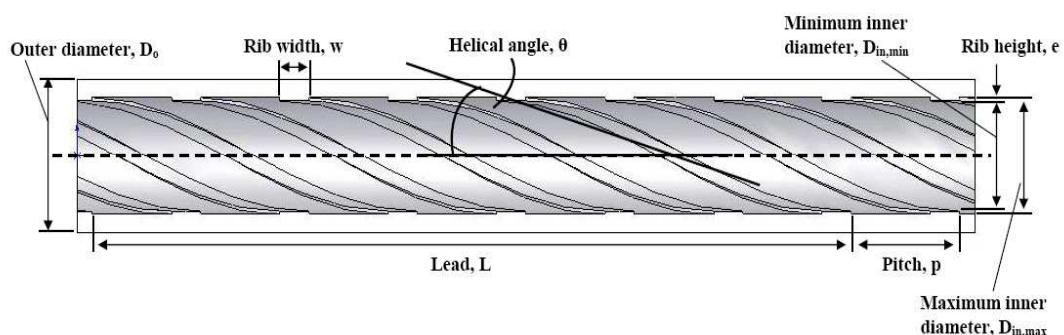


Figure 3.2 The geometry parameters of the rifled tube which is modeled in the Solidworks®.

Table 3.1 The dimension of the rifled tube geometry parameters.

Tube type	Rifled tube
Outer diameter, D_o (mm)	45.0
Maximum inner diameter, $D_{in,max}$ (mm)	34.1
Minimum inner diameter, $D_{in,min}$ (mm)	32.1
Equivalent inner diameter, D_{eq} (mm)	33.1
Rib height, e (mm)	1.0
Rib width, w (mm)	9.3
Helix angle, θ ($^\circ$)	26
Number of starts	6

The smooth tube which is modeled in the present study has the outer diameter 45.0 mm and inner diameter 34.1 mm.

In the present study, since there is not heating condition at the outer wall, thus only the flow or fluid domain inside the rifled tube and smooth tube are modeled while the solid domain (or the wall) is neglected as shown in Figure 3.3. The fluid domain inside the rifled tube and smooth tube has been modeled in Solidworks® in 3 dimensional with length of 2 meter long. It is assumed that both of the rifled tube and smooth tube are made of carbon silicon steel ($Mn < 0.1\%$, $0.1\% < Si \leq 0.6\%$) (Çengel, Y. A., 2003).

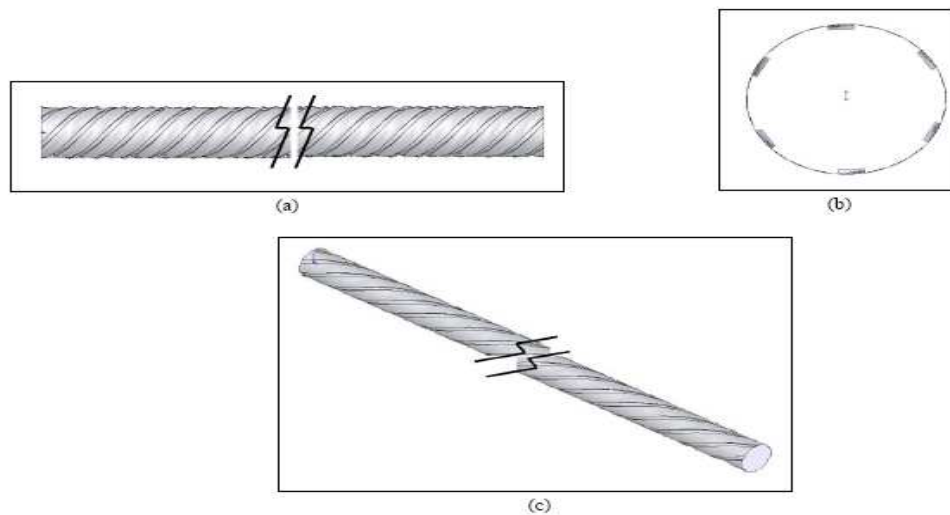


Figure 3.3 A 3-dimensional fluid domain of the rifled tube which is modeled in the Solidworks®.

3.3 Pre-processing

3.3.1 Meshing

The control volume model (fluid domain inside the rifled tube) is meshed in the pre-processor software, i.e. Gambit®. An structured (block-structured) non-uniform grid system is used to discretize the governing equations. A typical hexahedral element (Figure 3.4) with eight nodes is used for the three-dimensional grid system of the control volume (Gambit® 2.4 electronic documentation). Figure 3.5 shows the meshing grid topology on isometric view of the rifled tube and smooth tube.

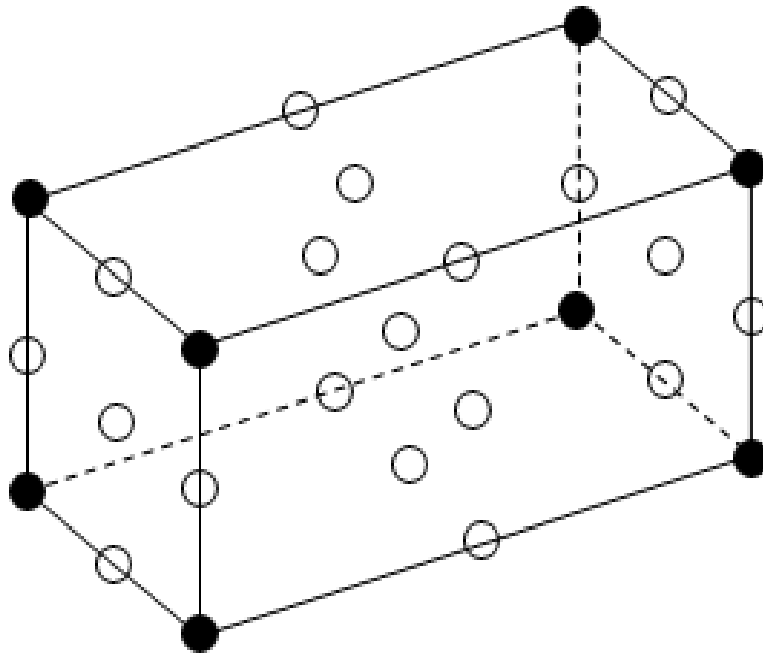
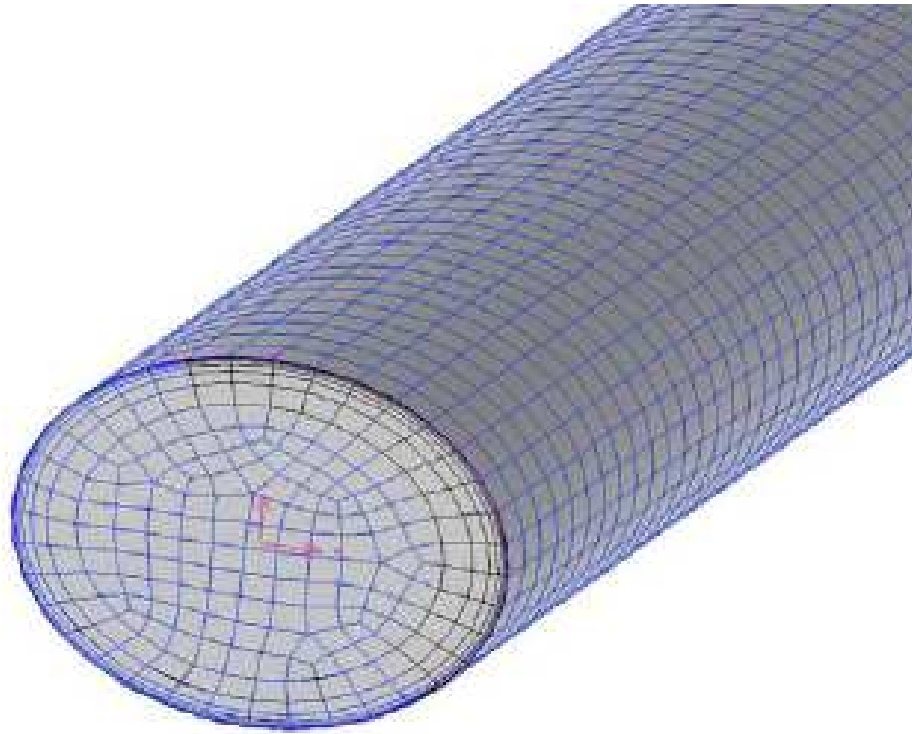
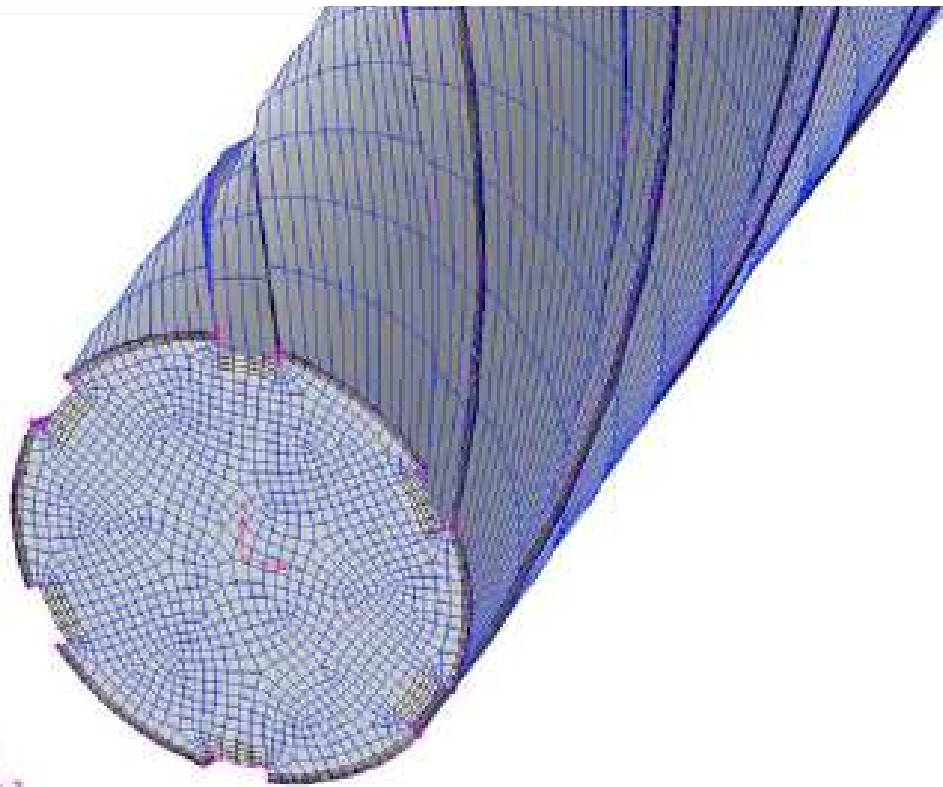


Figure 3.4 A typical hexahedral element with eight nodes (in black dote) which is used for storage of dependent variables. (Gambit® 2.4 electronic documentation)



(a)



(b)

Figure 3.5 The hexahedral mesh element is applied to the whole control volume of (a) smooth tube and (b) rifled tube.

3.3.2 Boundary condition

At the inlet of the smooth tube and rifled tube, it is assumed that the fluid which is water enters at room temperature, T_{in} 300K. The Reynolds number in the present study is ranging from $2.0 \times 10^4 - 1.4 \times 10^5$ and the flow is assumed to be flowing at atmospheric pressure. The setting at the inlet for the present study is as shown in Figure 3.6. Since velocity magnitude is needed, the value of the velocity magnitude has been calculated by using following equation;

$$u = \frac{Re \times \mu_f}{\rho_f \times D_h} \quad (4)$$

Since it is assumed that the flow in the smooth tube and rifled tube are fully developed turbulent flow, thus in the inlet panel (Figure 3.6), the turbulent intensity and hydraulic diameter are chosen as the Turbulence Specification Method. The turbulent intensity can be calculated by using following equation; (Fluent® 6.3 electronic documentation)

$$\text{Turbulent Intensity, } I = 0.16 \left(Re_D \right)^{1/8} \quad (5)$$

While the hydraulic diameter of the smooth tube and the rifled tube can be calculated using following equation;

$$\text{Hydraulic diameter, } D_h = \frac{4A_c}{P} \quad (6)$$

Where A_c is the cross section area of the tube and P is its perimeter. In the present study, the smooth tube hydraulic diameter is equivalent to its inner diameter which is 34.1mm. While for the rifled tube its hydraulic diameter is obtained as 30.16mm. The hydraulic diameter for the rifled tube is calculated as shown in Appendix K.

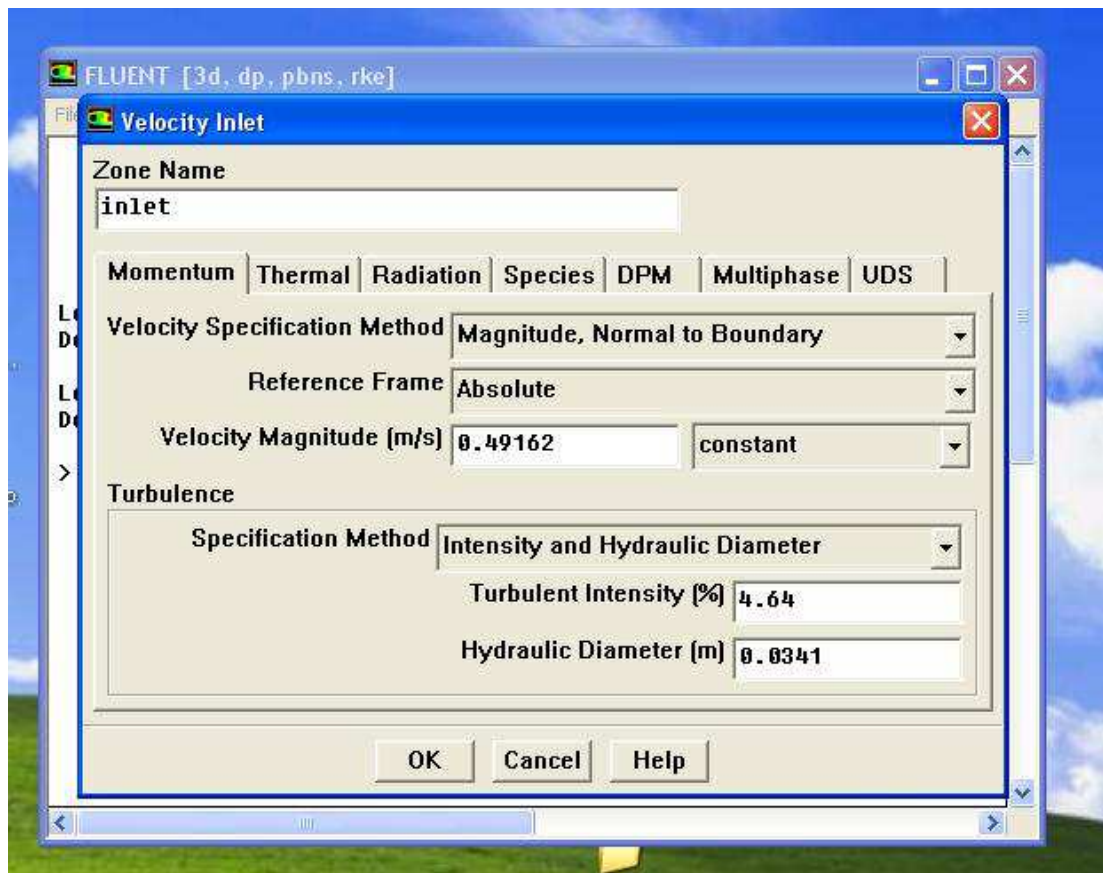


Figure 3.6 The setting at the inlet for the smooth tube and rifled tube.

In the present study, the flow is considered to be in steady state condition and since there is no uniform heating on the outer wall of the tubes, constant fluid properties such as density and viscosity is used. No slip boundary condition, $u_w = 0$ is imposed on the inner wall which is as shown in Figure 3.7.

REFERENCE

1. Cheng, L. X. & Chen, T. K. (2007) Study of vapor liquid two-phase frictional pressure drop in a vertical heated spirally internally ribbed tube. *Chemical Engineering Science*, Vol. 62, No. 3, pp. 783-792 [online version via <http://www.sciencedirect.com/science/article/B6TFK-4M6HY92-3/2/d3db42789cbc6cf0a4de9a4913b25f04>]
2. Cheng, L. & Xia, G. (2002) Experimental study of CHF in a spirally internally ribbed tube under the condition of high pressures. *International Journal of Thermal Sciences*, Vol. 41, No. 4, pp. 396-400 [online version via <http://www.sciencedirect.com/science/article/B6VT1-45625Y5-6/2/bfe75f178408435f3e854e1a5f80b6f4>]
3. Kim, C. H. et al. (2005) Critical heat flux performance for flow boiling of R-134a in vertical uniformly heated smooth tube and rifled tubes. *International Journal of Heat and Mass Transfer*, Vol. 48, No. 14, pp. 2868-2877 [online version via <http://www.sciencedirect.com/science/article/B6V3H-4G0YTK6-1/2/e6222885924aa908a25eb2d6c870e585>]
4. Tucakovic, D. R. et al. (2007) Thermal- hydraulic analysis of a steam boiler with rifled evaporating tubes. *Applied Thermal Engineering*, Vol. 27, No. 2-3, pp. 509-519 [online version via <http://www.sciencedirect.com/science/article/B6V1Y-4KNKH2N-3/2/42ffd5639f5a8bac73a704e7753abc45>]

5. Zarnett, G. D. & Charles, M. E. (1969). Cocurrent gas-liquid flow in horizontal tubes with internal spiral ribs. *The Canadian Journal of Chemical Engineering*, Vol. 47, pp. 238-241.
6. Cheng, L. X. and Chen, T. K. (2006). Study of single phase flow heat transfer and friction pressure drop in a spiral internally ribbed tube. *Chemical Engineering Technology*, Vol. 29, No.5, pp. 588-595.
7. Köhler, W. and Kastner, W. (1986). Heat transfer and pressure loss in rifled tube. *Proceeding of 8th International Heat Transfer Conference*, Vol. 5, pp. 2861-2865.
8. Webb, R. L. & Kim, N. H. (2005) *Principles of Enhanced Heat Transfer*. Boca Raton: Taylor & Francis.
9. Kundu, P. K. & Cohen, I. M. (2004) *Fluid Mechanics*. California: Elsevier Academic Press.
10. Çengel, Y. A. (2003). Heat transfer a practical approach. Boston: McGraw Hill. 2nd Edition.
11. Gambit® 2.4 electronic documentation.
12. Fluent® 6.3 electronic documentation.
13. Iwabuchi, M. et. al. (1982). Heat Transfer Characteristic of Rifled Tubes in the Near Critical Pressure Region. *Proceeding of 7th International Heat Transfer Conference*, Vol.5, pp. 313-318.
14. Cebeci, T. (2002). Convective Heat Transfer. Long Beach: Horizons Publishing. 2nd Revised Edition.

15. Lee, S. K. et. al. (2008). Experimental Study of Post-Dryout with R-134a Upward Flow in Smooth Tube and Rifled Tubes. *International Journal of Heat and Mass Transfer*, Vol. 51, pp. 3153-3163.
16. Henry, F. S. and Collins, M. W. (1991). Prediction of Flow over Helically Ribbed Surfaces. *International Journal for Numerical Methods in Fluid*, Vol.13, pp. 321-340.
17. Chandra, P. R. et al. (1997). Turbulent Flow Heat Transfer and Friction in a Rectangular Channel with Varying Numbers of Ribbed Walls. *Journal of Turbomachinery*, Vol.119, pp. 374-380.
18. Webb, R. L. et al. (1971). Heat Transfer and Friction in Tubes with Repeated Rib Roughness. *International Journal of Heat and Mass Transfer*, Vol. 14, pp. 601-617.
19. Smith, J. W. et al. (1968). Turbulent Heat Transfer and Temperature Profiles in a Rifled Pipe. *Chemical Engineering Science*, Vol. 23, pp. 751-758.
20. Cheng, L. X. and Chen, T. K. (2001). Flow Boiling Heat Transfer in a Vertical Spirally Internally Ribbed Tube. *Heat and Mass Transfer*, Vol. 37, pp. 229-236.
21. Almeida, J. A. and Souza Mendes, P. R. (1992). Local and Average Transport Coefficients for the Turbulent Flow in Internally Ribbed Tubes. *Experimental Thermal and Fluid Science*, Vol. 5, pp. 513-523.
22. Han, J. C. et al. (1978). An Investigation of Heat Transfer and Friction for Rib-Roughened Surfaces. *International Journal of Heat and Mass Transfer*, Vol. 21, pp. 1143-1156.

23. Yanaoka, H. et al. (2007). Numerical Simulation of Separated Flow Transition and Heat Transfer Around a Two-Dimensional Rib. *Heat Transfer - Asian Research*, Vol. 36, No. 8, pp. 513-528.

24. Weisman, J. et al. (1994). Two-Phase (Air-Water) Flow Patterns and Pressure Drop in the Presence of Helical Wire Ribs. *International Journal Multiphase Flow*, Vol. 20, No. 5, pp. 885-899.